



SAR reduction of wearable SWB antenna using FSS for wireless body area network applications

DIPIKA SAGNE*[✉] and RASHMI A PANDHARE[✉]

Department of Electronics and Communication Engineering, Indian Institute of Information Technology, Nagpur, India
e-mail: deepika.sagne@gmail.com; rush9ap@gmail.com

MS received 4 August 2023; revised 20 November 2023; accepted 23 November 2023

Abstract. A flexible Super Wide Band (SWB) antenna with a frequency selective surface (FSS) reflector is presented to reduce the specific absorption rate (SAR) and to improve the gain of the proposed antenna for Wireless Body Area Network (WBAN) Applications. A tapered feed circular monopole antenna with arrow-head-shaped slot structure is designed on Jeans substrate with a compact physical dimension of $22 \times 28 \times 0.3 \text{ mm}^3$. The use of a Jeans substrate makes the proposed antenna thin and highly flexible. The impedance bandwidth of the proposed antenna is 28 GHz (3.2–31.2 GHz) with a peak gain of 5.61 dBi. Since the antenna is intended for body wearable applications, its performance has been observed by placing the antenna near a human body phantom. This placement increased the SAR and reduced the gain. Further to reduce the SAR and to enhance the gain of the proposed SWB antenna a novel FSS reflector, which consists of a 2×2 array of elements, is located at a distance of 1.138λ (13 mm) below the proposed antenna. In order to reduce the SAR, the FSS array structure is placed between the antenna and the human's forearm. This placement reduced the specific absorption rate (SAR) by more than 95%. To make the proposed antenna with FSS structure user agreeable, the gap between the antenna and FSS is filled by polyethylene foam, with a dielectric constant of 2.26, a loss tangent of 0.00031, and a density of 2.2 lb. Further, there is also a 3–4 dBi improvement in antenna gain after the application of the FSS. The proposed antenna has great potential to be applied in human microwave imaging due to its immense wide bandwidth, high gain and compact size, and low SAR value.

Keywords. Conformal; FSS; jeans substrate; SAR; SWB; WBAN.

1. Introduction

The growing popularity of commercial wearable technology has aroused the interest of various research improvements in the field of wearable sensing technologies as a result of recent developments in the field of contemporary wireless communication systems. Future Internet of Things (IoT) technology will change how gadgets communicate with wearable electronics, such as those with flexible antennas [1]. Hence, flexible antennas have consequently drawn a lot of interest. As a result, recent research has focused on various flexible antennas for biomedical and other applications [2, 3]. As a part of wireless body area network (WBAN) systems, wearable textile antennas have recently piqued the interest of researchers from both academia and industry due to the variety of applications they can be used for, including in security, health, and military settings [4]. The use of wearable textile antennas in WBAN applications is favored because they have significant benefits, including being lightweight, having great flexibility,

being cheap, having low production complexity, and being simple to integrate into the garment [5]. There have been a number of flexible and textile-wearable antenna layouts proposed recently. [6] describes a flexible, wearable antenna for WLAN applications that is constructed on a denim substrate and has notch characteristics. [7] describes a flexible textile antenna for body-centric wireless communications running in the 2.45 GHz industrial, scientific, and medical spectrum and employing FR4, denim cotton, and Teflon substrates. A multiband Fractal Koch dipole textile antenna for wearable applications is described in [8]. An innovative, small, dual-band, all-textile PIFA for wireless body area network applications is presented in [9]. Two textile-based antennas are suggested for IoT and body-centric communication applications. The radiating structure, comprised of conductive copper threads, was created using the sewing embroidery process, and the antennas were constructed on textile cotton material. Most of these antennas have poor gain or a narrow bandwidth. Moreover, the Federal Communications Commission (FCC) selected the ultra-wideband (UWB) frequency spectrum for WBAN systems in 2002 [10]. This UWB frequency range is

*For correspondence
Published online: 15 February 2024

typically preferred for WBAN systems to operate on. On the other hand, as a result of recent advancements in wireless technology, the next generation of communication systems requires an antenna that is small, inexpensive, light, efficient, low-power, portable, and must also be capable of working with high data rates and high-quality wireless connectivity. The necessity for high-data-rate wireless communication over short distances can be satisfied by the employment of ultra wideband (UWB) radio technology [11, 12]. Yet, because of its general applicability through both short- and long-distance data communication, super wideband (SWB) technology has received a significant amount of attention in recent years [13].

SWB technology includes all the sophisticated features of UWB and offers better channel capacity with a higher data rate and increased resolution [14]. Due to the recent developments in wireless technology, WBAN requires wearable wideband antennas that can exchange digital information with high data rates and high-quality wireless connectivity that can easily maintain reliable and high-performance communication for both short- and long-distance [15] by using the human body as a data network. Lately, various [16] SWB antenna configurations using different flexible materials have been investigated. [15] describes a novel conformal super wideband (SWB) wearable textile antenna. A flexible antenna is employed on a material named Dacron fabric whose substrate with a bandwidth of almost 35 GHz. The designed antenna has been investigated with conformal analysis in terms of return loss and radiation characteristics. [17] Present a Super Wide Band (SWB) antenna design and its performance evaluation. This antenna is made of textile material for body area network applications. In [18] a low-cost PET paper has been used to design SWB antenna for wearable medical applications, vehicular navigation systems, and any other applications that require flexibility. The designed antenna operated from 1.6 to 56.1 GHz. In [19], a compact SWB antenna is designed on a thin and flexible ultralam 3850 laminates with a physical dimension of $60 \times 40 \times 0.1 \text{ mm}^3$, and it uses a circular disc monopole structure. The designed antenna is thoroughly analyzed in terms of its reflection coefficient, radiation pattern, gain, radiation efficiency, and surface current for 5G application.

It has been observed that most of the UWB or SWB antennas created for body-worn applications have been found to function worse when placed in close proximity to the body in terms of gain, directionality, and efficiency. Moreover, placing an antenna on a body causes electromagnetic waves to enter the body more deeply, increasing the system-specific absorption rate (SAR) value and rendering the intended antenna unsuitable for body-worn applications. Also, a variety of flexible materials are used to design an antenna for on-body applications. However, to ensure the comfort of users, such on-body antennas need to be designed on flexible textile or plastic substrates. Moreover, textiles are excellent substrates for wearable antenna

designs because of their low dielectric permittivity, which widens the antenna impedance bandwidth [20].

Due to the rising popularity of wearable technology, particularly health monitoring systems, the market for flexible electronics is expanding. Hence, the antenna must offer improved channel capacity and a higher data rate in order to be designed for application in health monitoring systems. Furthermore, the antenna for on-body application needs to be flexible and conformal, taking into account that different areas of the human body have varying dimensions and curvatures [15]. Also, most importantly, the antenna's gain must be high, as wearable antennas have been shown to have poor gain, and the antenna's SAR must be low to avoid interactions with the body, which is the final and most crucial requirement.

To address all the above-mentioned issues, we proposed a compact, flexible Super Wide Band (SWB) antenna designed on a jeans substrate. The suggested antenna is compact and extremely flexible since it uses a Jeans substrate. The impedance bandwidth of the proposed antenna is 28 GHz (3.2–31.2 GHz) with a peak gain of 5.61 dBi. Since the antenna is intended for body wearable applications, a single-layer frequency selective surface (FSS) reflector is employed to reduce the specific absorption rate (SAR) and improve the gain of the proposed antenna for wireless body area network (WBAN) applications. A novel FSS reflector, consisting of a 2×2 array of elements, is located at a distance of 1.138λ (13 mm) below the proposed antenna. However, in order to observe the SAR reduction, the same FSS structure is placed between the antenna and the human's forearm. This placement reduced the specific absorption rate (SAR) by more than 95%. There is a 3–4 dBi improvement in antenna gain after the application of the FSS. The proposed antenna has great potential to be applied for WBAN applications not only for short range but also for long range, due to its wide bandwidth, high gain, compact size, low SAR value, and also for providing comfort to users with the use of polyethylene foam.

2. Antenna configuration

The proposed arrowhead slot Super Wide Band (SWB) antenna is illustrated in figure 1. The antenna is designed on a Jeans substrate with a relative permittivity (ϵ_r) of 1.6, a loss tangent ($\tan \delta$) of 0.002, and a thickness of 0.3 mm. The overall dimensions of the substrate are $W_s \times L_s \text{ mm}^2$. To boost antenna performance and achieve 50-ohm impedance matching, a tapered connection is placed between the feed line and the main radiating patch. The optimized design parameters of the proposed SWB antenna have been depicted in table 1. The radius of a circular patch antenna 'R' is calculated using the Equation (1) [21, 22].

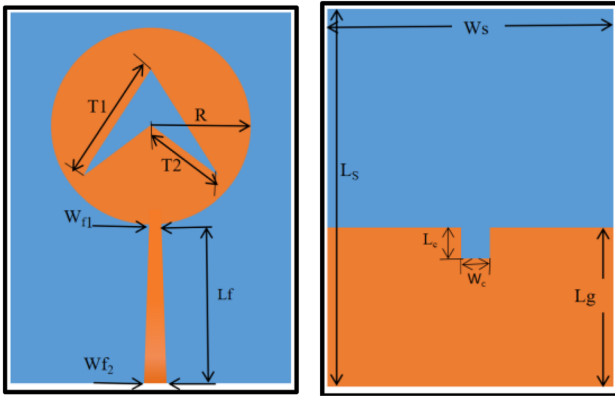


Figure 1. Arrow head slot super wide band (SWB) antenna.

$$f_L = \frac{7.2}{(L_g + R + p)} \text{GHz} \quad (1)$$

The design of the SWB antenna starts with a simple circular monopole antenna, as it's a basic technique to get wide and ultra-wide bandwidth, and the antenna is fed with a tapered feed line, as it provides good impedance matching. The rectangular DGS structure is inserted in the ground plane with the added inductive effect, thereby neutralizing the capacitive effect, and the antenna becomes more resistive, increasing the impedance bandwidth. Finally, the arrowhead structure is removed from the circular patch antenna as it increases the current density in the patch and enhances the bandwidth. The bandwidth of the designed antenna with the jeans substrate was achieved from 3.2 GHz to 31.2 GHz, as shown in figure 2. The gain varies from 3.87 to 5.61 dBi. The antenna achieves good bandwidth but has variable gain and continuously decreasing efficiency with frequency, i.e., from 0.65 to 0.78, as shown in figure 3.

3. SWB antenna impact on human body

Because the antenna is intended for body wearable applications, its performance should be evaluated by implanting the antenna near a human body phantom, as the body absorbs and reflects some electromagnetic energy. Figure 4

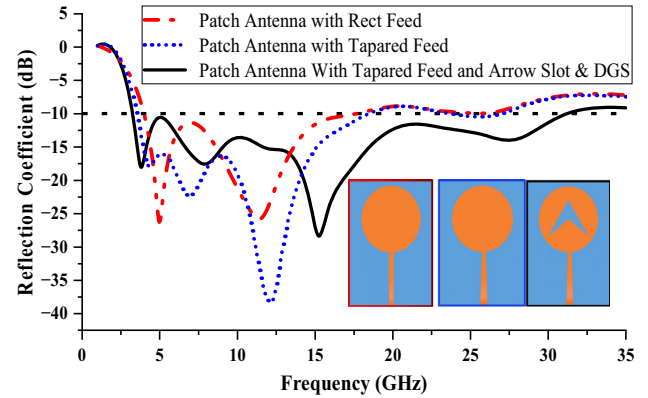


Figure 2. Simulated return losses of antenna with respect to stage-wise modification.

shows the phantom model for a hand structure. The designed body phantom has five layers. The last three layers are muscle, fat, and skin, and the inner two layers consist of bone layers such as cortical (80% of the total skeleton dimension) and cancellous (20% of the total skeleton dimension) [23–25].

For the layers of a body phantom that represent the muscle, fat, skin, bone (cancellous), and bone (cortical), the dielectric and thermal characteristics with regard to frequencies are taken into account. Table 2 below [26], where ‘ ϵ ’ is permittivity and ‘ σ ’ is the electrical conductivity in S/m, gives the specific dielectric parameters for each layer with respect to frequency.

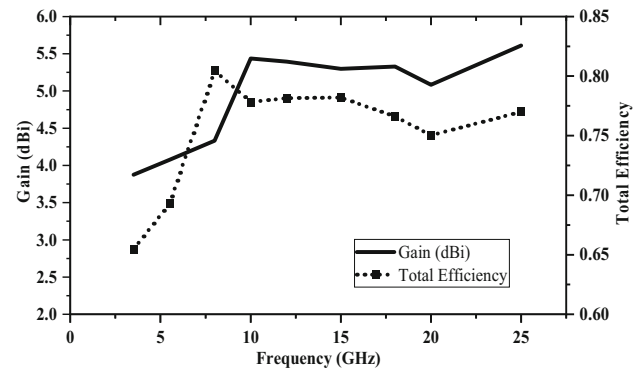


Figure 3. Antenna Gain and Efficiency plot with respect to frequency.

Table 1. Parameters of the proposed SWB antenna.

Parameters	Dimensions (mm)	Parameters	Dimensions (mm)	Parameters	Dimensions (mm)
Substrate width (W_s)	22	Feed width (W_{f1})	1.5	Feed width (W_{f2})	0.7
Substrate length (L_s)	28	Slot length (L_s)	1	Length (T_1)	12.7
Ground plane Length (L_g)	10.25	Slot width (W_s)	1	Length (T_2)	6.9
Radius of patch (R)	8.5	Feed length (L_f)	10.5	Antenna height (h)	0.3

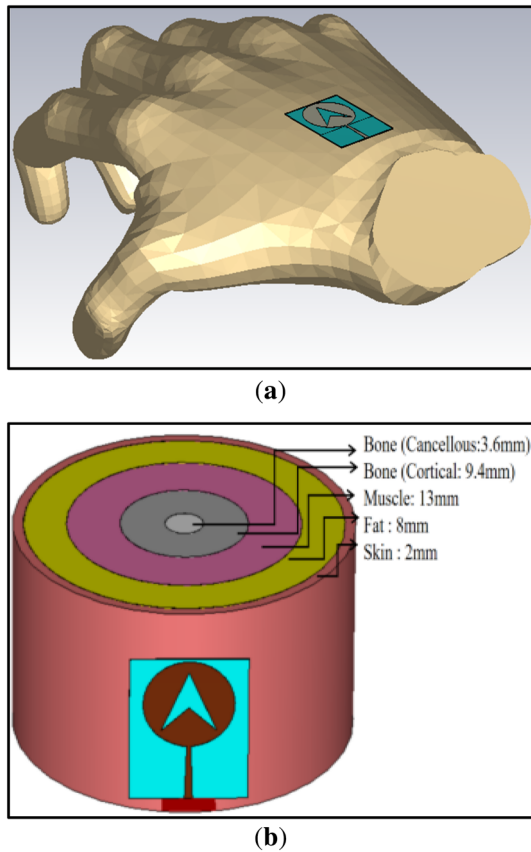


Figure 4. Proposed antenna on the phantom model for a hand structure.

The phantom model has been designed by considering the dielectric properties of each phantom layer for different frequencies, as shown in table 2. Further, the SAR study has been carried out by implanting the antenna 14 mm away from the human body phantom [27], in order to examine the effect of the proposed antenna on the human body, as illustrated in figure 5. The International Commission on Non-Ionizing Radiation Protection imposes regulatory limitations to safeguard the human body from the effects of hazardous radiation. The maximum SAR value for 1 gm of

tissue, is 1.6 W/Kg, and for 10 gm of tissue, it is 2 W/Kg according to regulatory criteria.

Table 3 displays the SAR values for 1 gm and 10 gm tissues determined for various frequencies within the proposed SWB antenna bandwidth range. As shown in table 3 below, it has been found that placing an antenna on a person results in electromagnetic waves penetrating the body more deeply, raising the system-specific absorption rate (SAR) value and decreasing the gain.

The system-specific absorption rate (SAR) value rises when an antenna is placed near or directly over a person's body. The interface between the antenna and body should be avoided in order to lower the SAR value. One strategy is to integrate Frequency Selective Surface (FSS) structures at the back of the antenna to prevent the antenna from coming into direct contact with the body. As a result, the FSS structure is used as a reflector, as an extra effort to lower the SAR values to safe levels and also to enhance the gain [24, 25], as detailed in the section below.

4. SWB antenna with FSS structure

Figure 6 depicts the proposed FSS unit cell's geometry, and table 4 lists the optimum design parameters for the proposed FSS unit cell. The FSS structure is printed on the RT Duroid substrate with a thickness of 0.254, a permittivity ' ϵ_r ' of 2.2, and a loss tangent of 0.0009. It consists of three metallic square loop structures and four dipole elements. The unit cell (L1) dimension of FSS can be calculated approximately from Equation (2) as given below [27].

$$L1 = \frac{c}{4f_L \sqrt{(\epsilon_r + 1)}/2} \quad (2)$$

The FSS is designed in three steps, as shown in figure 7, in order to achieve a wider bandwidth in the SWB range. Initially, a square loop along with four slots at each corner provides the bandwidth from 4.75 GHz to 23 GHz. Further to enhance the bandwidth, a square with a phase shift of 45 degrees has been added to the design in step 2, and the FSS starts resonating from 4.2 GHz to 25 GHz. At last, another

Table 2. Dielectric properties of body phantom layers.

Tissue Dielectric properties	Skin		Fat		Muscle		Bone (Cancelous)		Bone (Cortical)	
	ϵ	σ	ϵ	σ	ϵ	σ	ϵ	σ	ϵ	σ
5.5 GHz	35.4	3.46	9.94	0.77	48.9	4.61	15.6	2.02	9.81	1.08
8.0 GHz	33.2	5.82	9.28	1.28	45.5	7.8	13.8	3.06	8.79	1.68
10 GHz	31.3	8.01	8.8	1.71	42.8	10.6	12.7	3.86	8.12	2.14
12 GHz	29.3	10.3	8.37	2.14	40.1	13.6	11.7	4.6	7.56	2.56
15 GHz	26.4	13.8	7.79	2.76	36.4	17.9	10.5	5.62	6.87	3.14
18 GHz	23.6	17.2	7.3	3.35	33	22.1	9.55	6.52	6.33	3.64
20 GHz	22	19.2	7.01	3.72	31	24.7	9.03	7.06	6.03	3.94
25 GHz	18.3	23.6	6.4	4.58	26.6	30.5	8	8.25	5.44	4.6

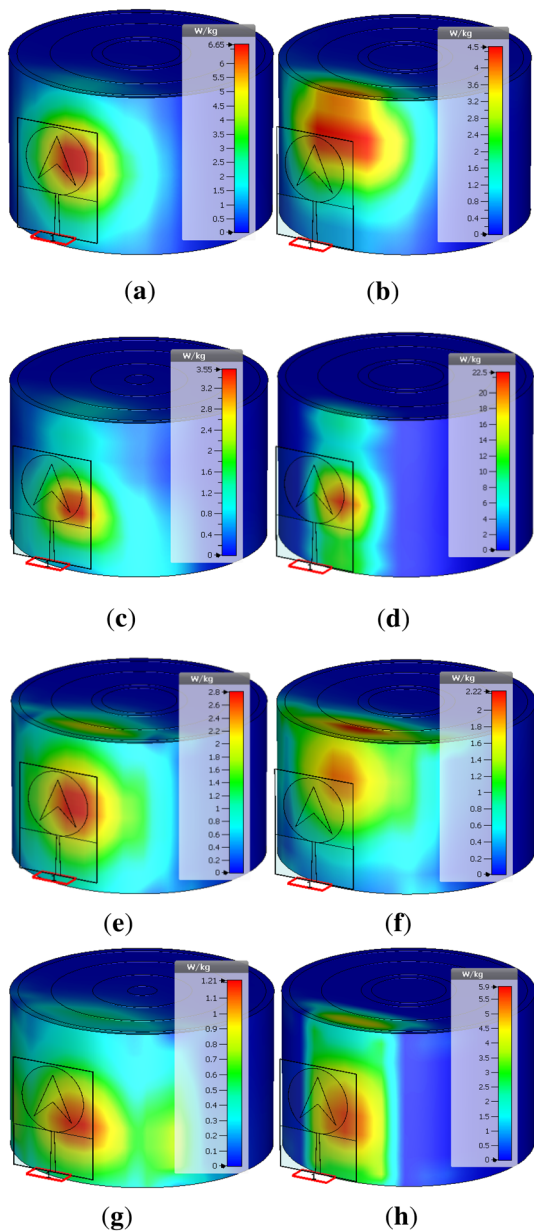


Figure 5. Proposed antenna on a human body phantom for SAR calculation for 5.5 GHz, 8 GHz, 12 GHz, and 20 GHz for 1 gm (a), (b), (c), (d) and 10 gm (e), (f), (g), (h), respectively.

square is inserted in order to improve surface current, which shifts the lower frequency to 3.05 GHz and increases the transmission characteristic bandwidth in the frequency range of 3.05 GHz to 28 GHz. The comparison of the transmission coefficients of FSS structures is shown in figure 8.

The 2×2 FSS array of dimensions $38 \times 38 \times 0.254$ mm³ is shown in figure 9. The proposed FSS array arrangement sets it behind the antenna in order to keep it away from the body, as seen in figure 10. The FSS is situated behind the antenna and optimised so that the reflected wave from the FSS and the transmitted wave from the

antenna are in phase [28, 29] in order to reduce the SAR value and achieve the gain increase.

The FSS, which is placed behind the antenna, impairs electromagnetic performance. The simulated reflection coefficient with and without FSS are contrasted in figure 11. The impedance bandwidth is unaffected by the application of FSS, but placing FSS with an antenna causes a negligible variation.

5. Antenna with FSS analysis for on-body scenario

It has been noted that the suggested antenna's impedance bandwidth is unaffected by the use of FSS. Further, the performance analysis of the suggested antenna with FSS has been carried out in terms of placement of the antenna with FSS and conformal analysis in this section to make the antenna appropriate for on-body use.

5.1 Placement of antenna with FSS

As depicted in figure 10, the FSS is positioned 0.138λ beneath the antenna. Merely air fills the space between the antenna and the FSS construction. To test the antenna performance with FSS in an on-body situation, this positioning is ineffective. To maintain this set distance between the antenna and the FSS, a metallic enclosure must be used. Unfortunately, the performance of the antenna may be negatively impacted by this metallic housing, and users may find it uncomfortable. In order to make the proposed antenna fully suitable for body-worn applications with user comfort, the gap between the antenna and FSS is filled by polyethylene foam, with a dielectric constant of 2.26, a loss tangent of 0.00031, and a density of 2.2 lb [30] as shown in figure 12(a). The antenna is located on top of the polyethylene foam, and at the bottom of the foam, the FSS structure is placed. Further, the belt has also been attached to the FSS structure to wear a complete antenna directly on hand as shown in figure 12(b).

Figure 13 compares the simulation of an antenna's reflection coefficient with FSS when the gap is filled with polyethylene foam and when it is filled with air. It has been observed that the use of polyethylene foam between the antenna and FSS has no impact on the impedance bandwidth.

5.2 Conformal analysis of antenna with FSS

Considering that different parts of the human body have distinct dimensions and curves, the antenna for on-body use needs to be flexible and conformal [20]. Due to its design on a denim substrate, the suggested antenna is completely flexible. To make the proposed antenna appropriate for mounting on a human body with different dimensions and

Table 3. SAR values of patch antenna at different stages (14 mm from the body).

Sl. No.	Frequency (GHz)	SAR (1gm)	SAR (10 gm)	Gain (dBi)
1	5.5	6.65	2.8	2.89
2	8	4.5	2.22	4.16
3	10	5.08	2.01	4.53
4	12	6.82	2.06	2.54
5	15	3.55	1.21	3.4
6	18	8.76	3.1	3.84
7	20	22.5	5.9	3.7
8	25	11.1	2.05	4.13

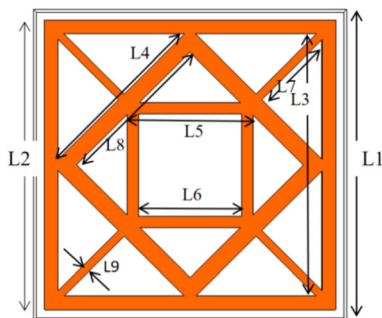


Figure 6. Configuration of the proposed FSS.

Table 4. Parameters of proposed FSS.

Parameter	Value	Parameter	Value
L1	19	L5	8
L2	18	L6	6.4
L3	16.5	L7	5.4
L4	11.5	L8	9.9
L9	0.5	L10	0.2

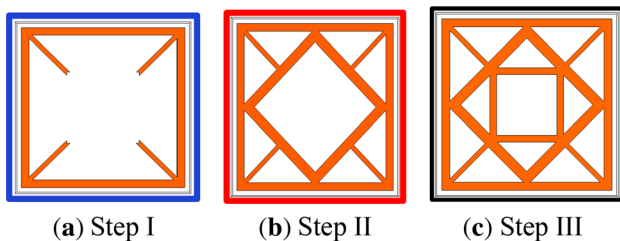


Figure 7. Step-wise modification of the proposed FSS.

curvatures, a conformal analysis of the designed antenna is also required. Several bending possibilities have been considered in the conformal analysis. As shown in

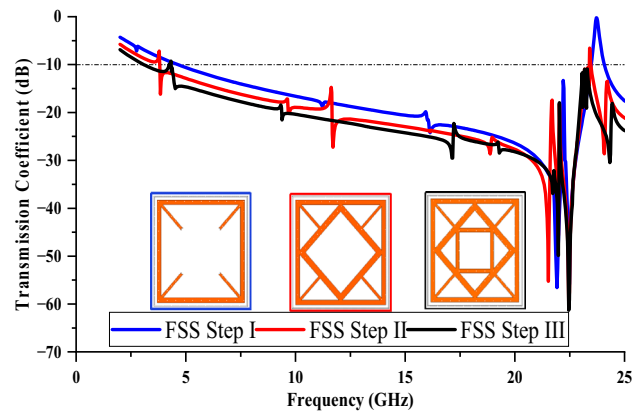


Figure 8. Transmission characteristics of square loop FSS and proposed FSS.

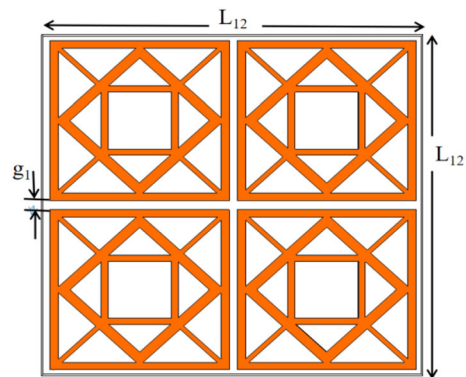


Figure 9. Array of unit cell FSS.

figure 14, the performance of the suggested antenna has been tested at various bending angles of 20°, 40°, and 60°.

Figure 15 illustrates the characteristics of an antenna's reflection coefficient with and without bending. It has a very slight effect on higher frequencies because it has been observed that as the bending angle increases, the higher frequency shifts slightly to the lower side. The bending analysis has been done for a complete structure, i.e., an

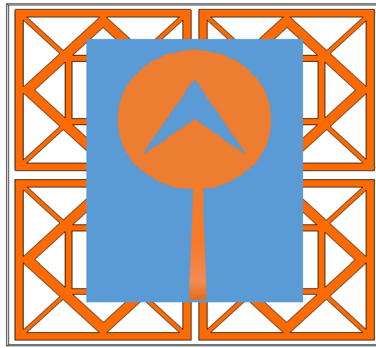


Figure 10. Front view of antenna integrated with FSS.

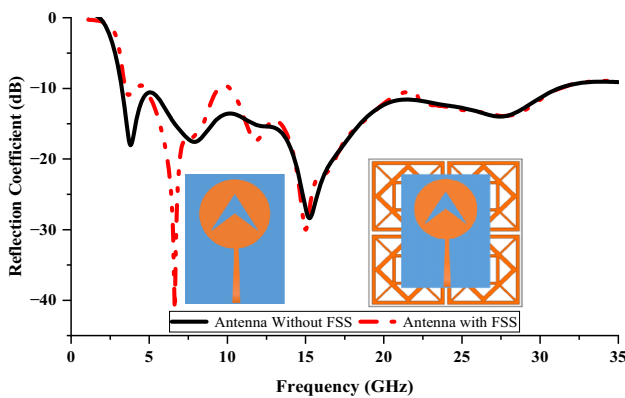


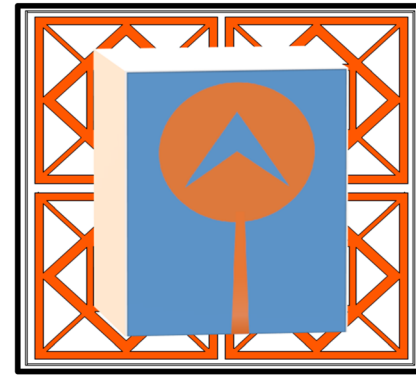
Figure 11. Front view of antenna integrated with FSS.

antenna with FSS along with foam in between to ensure the complete structure’s placement on the human body.

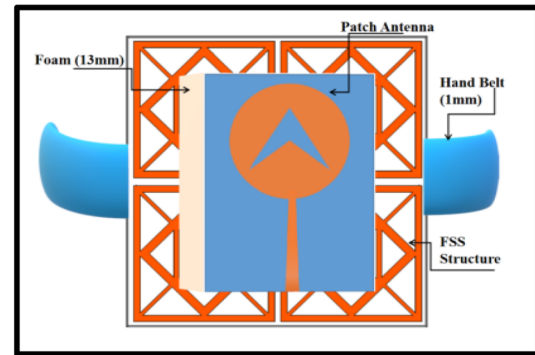
6. SAR and gain analysis of antenna using phantom model

Because of the direct interface between the antenna and the body, part of the electromagnetic energy radiated from the antenna is absorbed and part of it is reflected by the body [31], hence the SAR value increases above acceptable levels and the antenna gain also decreases, as shown in table 3. By integrating the suggested FSS structure between the body and antenna, as shown in figure 16, the direct interface between the antenna and body has been eliminated. Investigating the performance modification of the suggested antenna with FSS and its impact on the human body is crucial for on-body applications, hence further simulation was carried out by placing the antenna with an FSS array on the phantom model for a hand structure.

The 2x2 array FSS is placed on the phantom model directly and the antenna is placed above 13 mm from the FSS. This placement is supported by filling the gap between the antenna and the FSS with polyethylene foam. SAR



(a)



(b)

Figure 12. (a) Front view of the antenna with FSS filled by polyethylene foam. (b) A complete wearable structure of the proposed antenna.

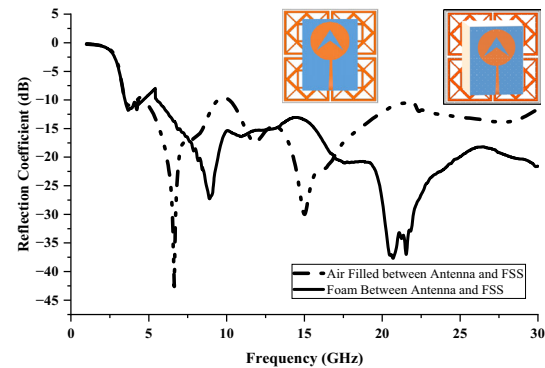


Figure 13. Comparative analysis of Return loss for gap filled with polyethylene foam and with air.

analysis has been carried out in order to examine the effect of the proposed antenna on the human body, as illustrated in figure 17. It has been observed that whenever the wave radiated towards the FSS is reflected back and added to the wave radiated from the antenna, If the two wave components are added in phase, then the back radiation is suppressed by integrating the FSS. The significant reduction in back radiation helps to achieve a lower SAR level [31, 32].

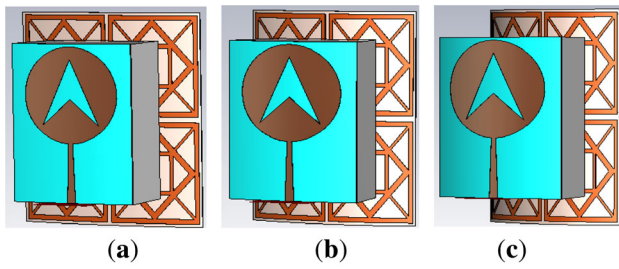


Figure 14. The proposed antenna with (a) 20°, (b) 40° and (c) 60° bending angles.

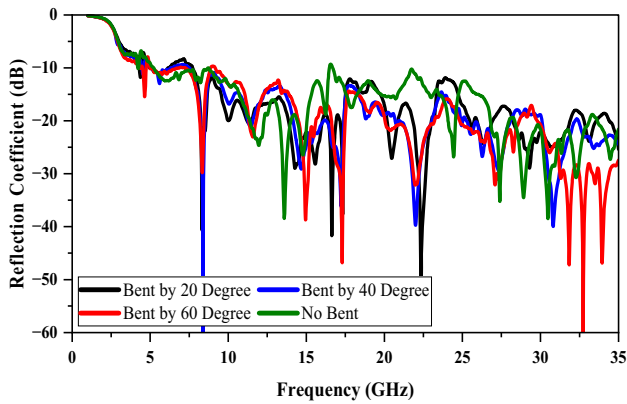


Figure 15. Proposed antenna reflection coefficient characteristics for bending angles.

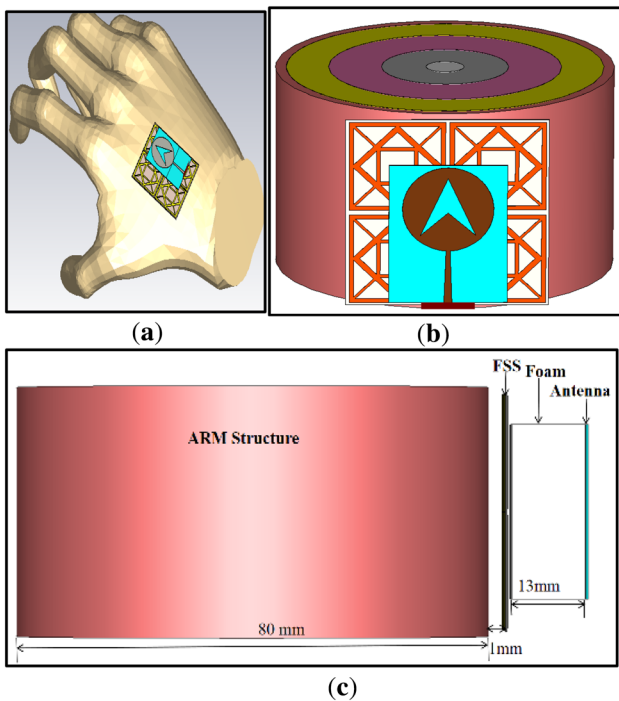


Figure 16. Antenna with FSS on (a) Hand structure, (b) On phantom model and (c) Side view.

According to regulatory criteria, the maximum SAR value for 1 gm of tissue is 2 W/kg, and for 10 gm of tissue, it is 1.6 W/kg. The SAR values of the SWB antenna with FSS of various stages for 1 gm and 10 gm tissues were calculated for various frequencies within the intended SWB antenna bandwidth range and are shown in table 5 for 1 gm and 10 gm tissues. The specific absorption rate (SAR) value has been found to decrease when an FSS is integrated between an antenna and a human body. The SAR obtained is below the FCC’s recommended level of 1.6 W/kg. The SAR is reduced by 95.45% compared to the antenna without FSS.

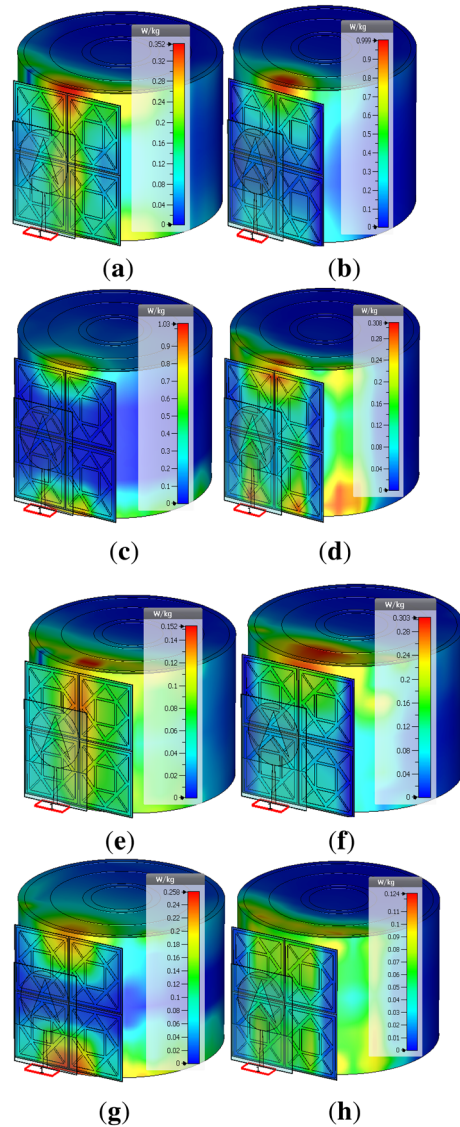


Figure 17. Proposed antenna with FSS on a human body phantom for SAR calculation for 5.5 GHz, 8 GHz, 15 GHz, 20 GHz for 1 gm (a), (b), (c), (d) and 10 gm (e), (f), (g) and (h) respectively.

Table 5 also shows that the FSS structure implemented with the antenna serves as a reflector [31, 33] and is responsible for increasing the antenna’s gain for on-body applications. As the radiated waves impinge on the FSS reflector, they reflect back, which in turn affects the antenna characteristics. The gain has been enhanced as the wave radiated by the antenna and the wave reflected from the FSS are in phase to enhance the antenna gain [29, 33].

Figure 18 shows a comparative analysis of gain and efficiency for the proposed SWB antenna without FSS, the antenna with FSS, and the proposed antenna with foam in between over the complete SWB range. The gain is increased by 48.12% as compared to an antenna without FSS. The gain for foam placed between the proposed antenna and FSS is near the same as for air filled between the antenna and FSS, and there is a slight enhancement in efficiency shown in figure 18(a). Efficiency is nearby constant for all the three cases shown in figure 18(b).

The suggested flexible SWB antenna with FSS is also contrasted with a few other flexible and semi-flexible antennas found in the literature in order to compare the proposed work with the literature already in existence. Table 6 depicts the comparison.

The proposed flexible SWB antenna has been compared mostly in terms of the SAR reduction technique used on flexible antennas for body wearable applications based on the literature. Further, the proposed antenna has also been compared in terms of size, percentage of bandwidth, conformal analysis, and peak gain for wearable applications, with most of the options available for body applications, as shown in table 6.

In [32], SAR reduction using FSS has been achieved. However, the size of the antenna is very large, and the bandwidth is very low. [34] shows SAR reduction using metamaterial; the bandwidth is in the UWB range, whereas the gain is less, and conformal analysis has not been performed. In [35], a dual-band antenna designed on polyamide substrates and metamaterials has been used for SAR reduction. However, the antenna can be used only for short-distance communication, and conformal analysis has not been performed. [36] used polyethylene foam to design a dual-band antenna with a very large size. In this work,

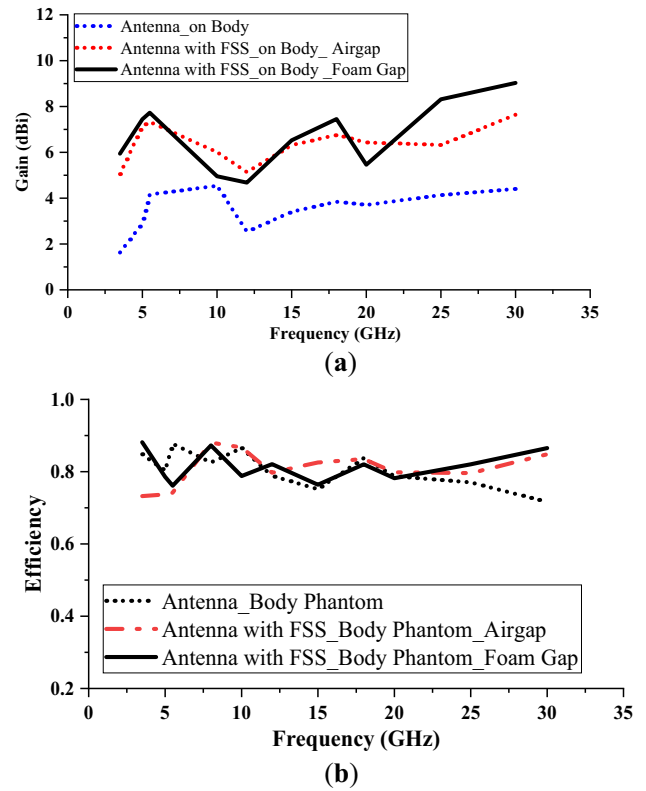


Figure 18. (a) Gain of the proposed antenna with and without FSS over the complete SWB range. (b) Efficiency of the proposed antenna with and without FSS over the complete SWB range.

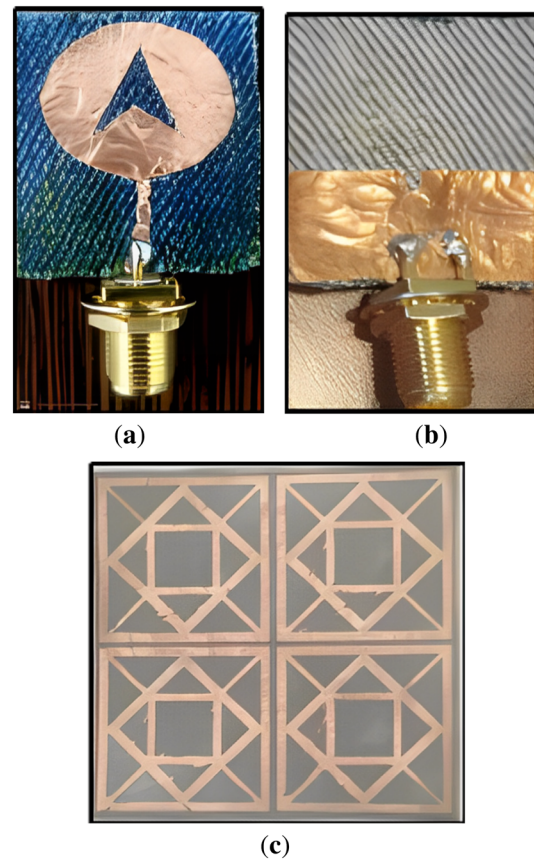
electromagnetic band gap (EBG) structures are used for SAR reduction, and antennas can be used for short-distance communication. In [37], a metal rim TP substrate was used to design a tri-band antenna and TCM of composite PEC-lossy dielectric structures used for SAR reduction. This antenna can be used only for short-distance communication, and conformal analysis has not been performed. [38] shows a UWB antenna using SAR reduction using a reflector. A backed UWB antenna has been performed. This antenna is not flexible, and hence conformal analysis has not been performed, and gain is also on the lower side.

Table 5. SAR Values of SWB antenna with FSS of different stages.

Sr. No.	Frequency (GHz)	SAR (1gm)	SAR (10 gm)	Peak Gain (dBi)
1	5.5	0.352	0.152	7.09
2	8	0.999	0.303	4.81
3	10	1.23	0.862	5.44
4	12	0.822	0.308	5.74
5	15	1.03	0.258	5.02
6	18	0.986	0.217	7.72
7	20	0.308	0.124	7.29
8	25	0.315	0.08	8.13

Table 6. Comparative analysis of the proposed SWB antenna with a few flexible antenna's available literature.

Ref. No.	Antenna dimension with reflectors (mm ²)	Frequency range GHz	Bandwidth %	Peak gain dBi	Material used	Conformal analysis	SAR analysis	Methodology for SAR reduction
[32]	120 × 120	2.07–2.62	23%	7.76	Jeans	Yes	Yes	Using FSS
[34]	100 × 100	4.55–13	96.29%	6	Felt	No	Yes	Using Metamaterial
[35]	42 × 42	2.4, 5.5	Dual Band	9.3	Polyamide	Yes	Yes	Using Metamaterial
[36]	176.5 × 176.5	2.5, 5.2	Dual Band	NA	foam	Yes	Yes	Using EBG structures
[37]	48.8 × 48.8	1.5-, 2.4, 3.4	Tri Band	NA	Metal Rim TP substrate	No	Yes	Using TCM of composite PEC-lossy Substrate
[38]	36 × 36	2.86–9.14	104.6%	5.82	FR4	No	Yes	Using Reflector Backed UWB antenna
Proposed	38 × 38	3.2 to 31.3	163%	8.31	Jeans	Yes	Yes	Using FSS of SWB antenna 95.45%

**Figure 19.** Fabricated Patch antenna (a) Front side, (b) back side and (c) FSS front side.

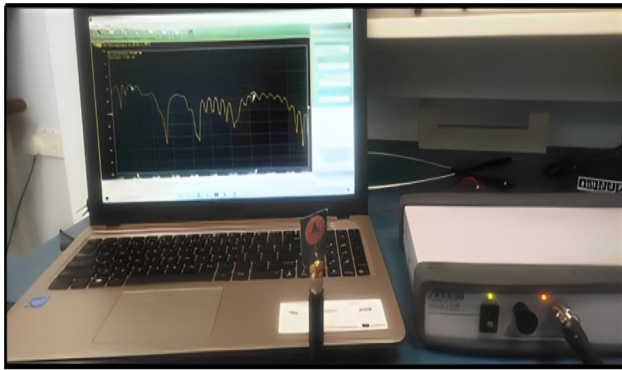
Finally, the proposed antenna designed on a flexible material shows a very compact size for a SWB range, and the FSS reflector is used to reduce the SAR and enhance the gain. The conformal analysis has also been performed, which makes the proposed antenna most suitable for wearable applications. According to a review of previously published work available in the open literature, no such work has yet been reported in which an SWB antenna was designed on a jeans substrate and used FSS for SAR reduction and gain enhancement.

The suggested flexible SWB antenna's compactness and superior performance characteristics in terms of size, bandwidth, flexibility, and SAR make it the most ideal antenna for a variety of WBAN and medical applications.

7. Measured results and discussion

7.1 Fabricated antenna and FSS with its measurement setup

The proposed SWB antenna is built on a Jeans substrate with a thickness of 0.3 mm and a thickness of 0.05 mm of copper tape, as shown in figures 19(a, b) below. The FSS structure is designed on an RT duroid substrate with a



(a)



(b)

Figure 20. Measurement set up for (a) Antenna with VNA for S11 and (b) Dielectric constant of Jeans Material.

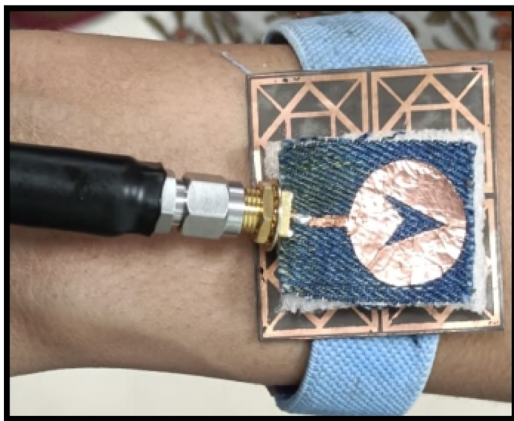


Figure 21. Fabricated patch antenna assembly.

thickness of 0.254 mm, as shown in figure 19(c). The measurement setup for the fabricated antenna is shown in figure 20. The MS46122B VNA up to 20 GHz is used to measure the reflection coefficient with Shockwave software

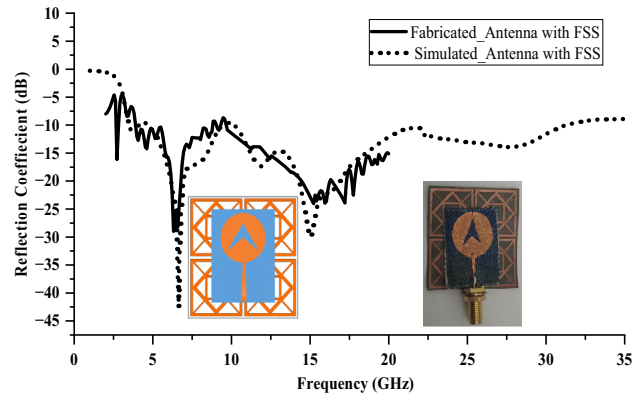


Figure 22. Return loss versus frequency graph for simulated and measured antenna with FSS.

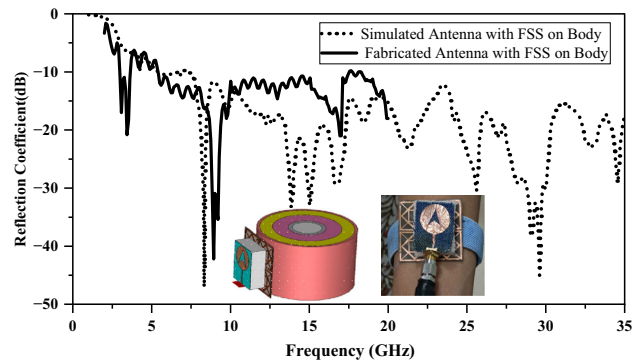


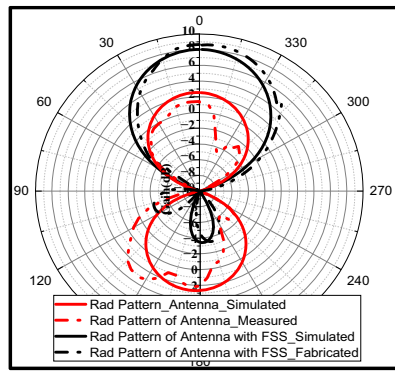
Figure 23. The return loss versus frequency graph for simulated and measured antenna.

on a laptop, as shown in figure 20(a). The results are measured using VNA for the various stages, i.e., only for SWB, SWB antenna with FSS, where air is in between FFS and antenna, and SWB antenna with FSS, where foam is in between FFS and antenna.

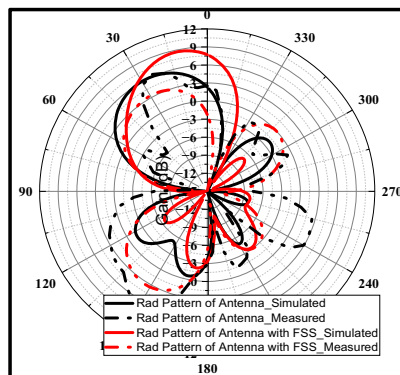
Figure 20(b) shows the setup measurement of the dielectric properties of the jeans material using the Keysight N1501A Dielectric Probe Measurement kit. Figure 21 shows the assembly of the designed antenna, which consists of a SWB antenna, FSS, foam, and a supporting belt for wearable purposes. The belt and foam are 1 mm and 13 mm thick, respectively. Foam is placed between the SWB antenna and the FSS structure. The whole assembly is mounted on a belt, as shown in figure 21.

Figure 22 shows the comparison result of the simulated and measured reflection coefficient graph of the antenna with the FSS array structure. Figure 23 shows the comparison graph of the reflection coefficient of patch antenna assembly for on-body applications for both simulated and fabricated cases.

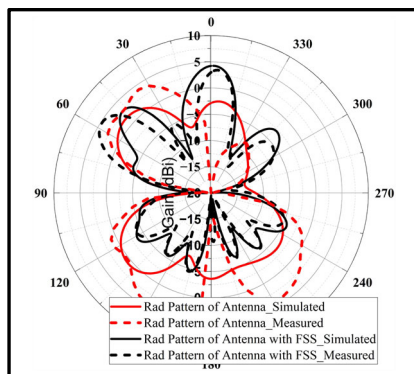
The suggested SWB antenna with FSS-simulated reflection coefficients (S11) is compared with the measured reflection coefficients in the body scenario in figure 23. The



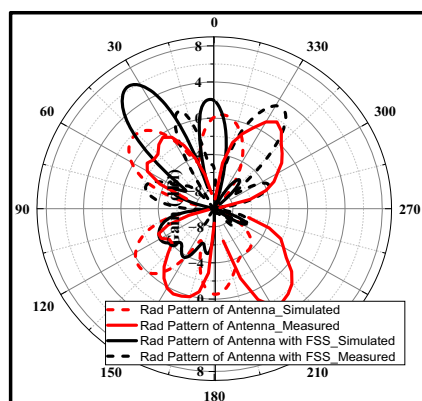
(a)



(b)



(c)



(d)

◀ **Figure 24.** Radiation pattern of the proposed antenna with and without FSS (a) 5 GHz, (b) 10 GHz, (c) 15 GHz and (d) 20 GHz.

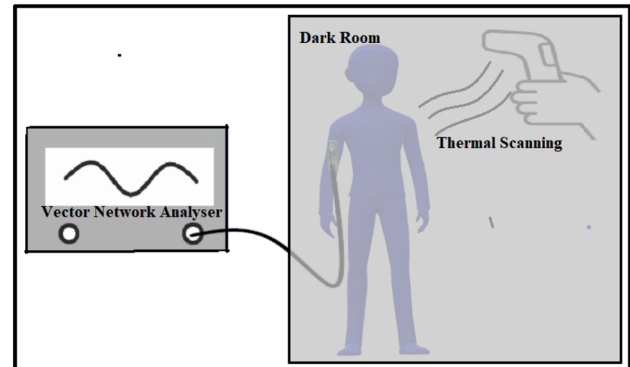


Figure 25. Thermal analysis arrangement for SAR measurement.

antenna resonates between 3.2 and 31.2 GHz, and the fabricated antenna has only been tested using the Vector Network Analyzer up to 20 GHz. The results from simulation and measurement have been found to be very close to each other. However, the tiny variation is brought on by a fabrication tolerance fault.

7.2 Radiation pattern

The comparative analysis of simulated and measured radiation patterns of the SWB antenna with and without FSS at 5 GHz, 10 GHz, 15 GHz, and 20 GHz are shown in figure 24(a), (b), (c), and (d) respectively. It can be seen that the antenna without FSS has almost stable radiation patterns that are nearly bidirectional in the E (Y-Z)-plane ($\phi = 90^\circ$) over the entire ultra wide band bandwidth. However, for the antenna with FSS nearly unidirectional radiation pattern in the E (Y-Z)-plane ($\phi = 90^\circ$). At higher frequencies, undesirable side lobes are generated with the main lobe due to the multi-directional current distribution and higher-order modes of excitation. The simulated and measured radiation patterns are found to be in close agreement. There is a slight difference due to measurement testing and alignment errors.

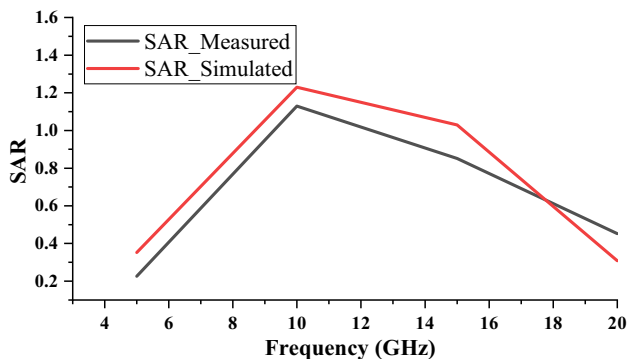
7.3 SAR measurement

The SAR measurement is possible by the following three methods [39].

1. Electric Field Distribution Measurement Method
2. Temperature Distribution Measurement Method
3. Magnetic Field Measurement Method

Table 7. Practical Measurement of SAR values using Thermal analysis.

Frequency (GHz)	Temperature		Temp. Change (ΔT)	Measured SAR Value	Simulated SAR Value
	Temp. at Initial Time	Temp. after 20 min			
5.5 GHz	35.6	35.7	0.1	0.226	0.352
10 GHz	35.6	36.0	0.4	1.13	1.23
15 GHz	35.6	35.9	0.3	0.851	1.03
20 GHz	35.6	35.8	0.2	0.452	0.308

**Figure 26.** A comparative analysis of measured and simulated SAR.

In this work, the Temperature Distribution Measurement Method has been used to calculate the SAR value practically. The thermal analysis method is used for the practical measurement of SAR values, where the antenna is placed on the human body and powered by VNA as a signal generator, as shown in figure 25.

In this method, thermal screening is used to calculate the change in temperature. The change in temperature is calculated after twenty minutes by considering the initial time, i.e., starting from zero for different frequencies as shown in table 7. Depending upon temperature change, SAR can be calculated using Equation (3) [32, 39].

$$\text{SAR} = c \frac{\Delta T}{\Delta t} \quad (3)$$

Where “c” is the heat capacity of the skin layer of the body phantom. The heat capacity of skin layers is 3391, for SAR analysis [26]. The thermal analysis is carried out to analyze the impact of radiation exposure of signal on the body, and consequently, changes in SAR values are observed. Table 7 shows the comparison between simulated and measured SAR values to judge the realistic performance of the proposed antenna.

Figure 26 shows the comparative analysis of measured and simulated SAR. It has been noted that there are slight changes in the measured and simulated SAR values. However, the measured SAR obtained is also below the FCC’s recommended level of 1.6 W/kg.

8. Conclusion

This paper designs and analyses a compact, fully flexible, arrowhead slot SWB antenna with FSS structure for body wearable applications. The impedance bandwidth of GHz (3.2–31.2 GHz) with a peak gain of 8.31 dBi has been achieved for a very compact physical dimension. In order to prove the relevance of the proposed antenna for wearable applications, SAR analysis has been performed. In order to reduce SAR, a compact FSS structure of $38 \times 38 \times 0.254 \text{ mm}^3$ was used, which reduced the SAR by 95.45% and enhanced the gain by 3–4 dBi compared to an antenna without FSS. The proposed SWB antenna is suitable for both short- and long-distance data communication with a fractional bandwidth of 162%. In addition to this, the flexibility and bending capabilities of the proposed antenna were also tested under different bending conditions and found suitable considering the distinct dimensions and curves of the human body. The use of foam material between the antenna and FSS makes the proposed antenna highly comfortable for wearing applications without any adverse effect on antenna performance. Furthermore, with the complete setup, the antenna’s efficiency has been increased. The proposed SWB flexible antenna with FSS maintaining low SAR, high gain, and efficiency with bending capabilities makes it highly suitable for body wearable applications with user comfort for both short- and long-distance data communication.

References

- [1] Hall Peter S and Hao Y 2012 Antennas and Propagation for Body-Centric Wireless Communications. 2nd edn. Artech House, London, UK, pp 1–7
- [2] Liu H, Wang J and Luo X 2017 Flexible and compact AMC based antenna for WBAN applications. In: *2017 IEEE International Symposium on Antennas and Propagation & USNC/URSI National Radio Science Meeting*. IEEE, pp. 587–588
- [3] Naik K K, Teja S C S, Sailaja B V and Sri P A 2020 Design of flexible parasitic element patch antenna for biomedical application. *Progress Electromag. Res. M* 94: 143–153

- [4] Shakhirul M S, Jusoh M, Sahadah A, Nor C M and Rahim H A 2014 Embroidered wearable textile antenna on bending and wet performances for UWB reception. *Microw. Opt. Technol. Lett.* 56: 2158–2163
- [5] Hassan S and Shehab S H 2015 Evaluation of an Ultra Wideband (UWB) textile antenna in the vicinity of human body model for WBAN applications. In: *2015 IEEE International WIE Conference on Electrical and Computer Engineering (WIECON-ECE)*. IEEE, pp. 195–198
- [6] Roy A, Biswas A K, Nandi A and Basu B 2023 Ultra-wideband flexible wearable antenna with notch characteristics for WLAN applications. *Progress Electromag. Res. C* 129: 143–155
- [7] Kavitha A and Swaminathan J N 2019 Design of flexible textile antenna using FR4, jeans cotton and teflon substrates. *Microsyst. Technol.* 25: 1311–1320
- [8] Jalil M E B, Abd Rahim M K, Samsuri N A, Murad N A, Majid H A and Kamardin K *et al.* 2013 Fractal koch multiband textile antenna performance with bending, wet conditions and on the human body. *Progress Electromag. Res.* 140: 633–652
- [9] Varma S, Sharma S, John M, Bharadwaj R, Dhawan A and Koul S K 2021 Design and performance analysis of compact wearable textile antennas for IoT and body-centric communication applications. *Int. J. Antennas Propag.* 1–12
- [10] Washington D C 2002 First Report and Order on Ultra-Wideband Technology. FCC, USA, pp 2–48
- [11] Yu W, Li W, Chang D C and Li Y 2014 Small antennas: miniaturization techniques and applications. *Int. J. Antennas Propag.* 1–7
- [12] Pandhare R A, Abegaonkar M P and Dhote C 2022 UWB antenna with novel FSS reflector for the enhancement of the gain and bandwidth. *Int. J. Antennas Propag.* 14: 1353–1368
- [13] Chen K R, Sim C Y D and Row J S 2011 A compact monopole antenna for super wideband applications. *IEEE Antennas Wirel. Propag. Lett.* 10: 488–491
- [14] Tran D, Aubry P, Szilagy A, Lager I E, Yarovy O and Lighthart L P 2010 On the design of a super wide band antenna. *Ultra Wideband* 17: 399–426
- [15] Mahmud S, Dey S and Saha N 2012 Super wide band wearable antenna: assessment of the conformal characteristics in terms of impedance matching and radiation properties. In: *2012 International Symposium on Antennas and Propagation (ISAP)*. IEEE, pp. 563–566
- [16] Santas J G, Alomainy A and Yang H 2007 Textile antennas for on-body communications: techniques and properties. In: *2nd European Conference on Antennas and Propagation (EuCAP 2007)*. Institution of Engineering and Technology, pp. 537–537
- [17] Mollah G, Shikder K and Arifin F 2020 Design and evaluation of a SWB decagonal patch textile antenna for WBAN applications. In: *2020 IEEE Region 10 Symposium (TENSYP)*. IEEE, pp. 1420–1423
- [18] Hasan Md R, Riheen M A, Sekhar P and Karacolak T 2020 Compact CPW-fed circular patch flexible antenna for super-wideband applications. *IET Microw. Antennas Propag.* 14: 1069–1073
- [19] Dey S, Arefin M S and Karmakar N C 2021 Design and experimental analysis of a novel compact and flexible super wide band antenna for 5G. *IEEE Access* 9: 46698–46708
- [20] Yalduz H, Tabaru T E, Kilic V T and Turkmen M 2020 Design and analysis of low profile and low SAR full-textile UWB wearable antenna with metamaterial for WBAN applications. *AEU Int. J. Electron. Commun.* 126: 153465
- [21] Ray K P and Ranga Y 2007 Ultrawideband printed elliptical monopole antennas. *IEEE Trans. Antennas Propag.* 55: 1189–1192
- [22] Ray K P and Tiwari S 2010 Ultra wideband printed hexagonal monopole antennas. *IET Microw. Antennas Propag.* 4: 437–445
- [23] Afridi A, Ullah S, Khan S, Ahmed A, Khalil A H and Tarar M A 2013 Design of dual band wearable antenna using metamaterials. *J. Microw. Power Electromag. Energy* 47: 126–137
- [24] Habibovic P and Barralet J E 2011 Bioinorganics and biomaterials: bone repair. *Acta Biomaterialia* 7: 3013–3026
- [25] Fuchs R K, Thompson W R and Warden S J 2019 Bone biology. In: *Bone Repair, Biomaterials*. Elsevier, pp. 15–52
- [26] Hasgall PA, Di Gennaro F, Baumgartner C, Neufeld E, Lloyd B, Gosselin MC, Payne D, Klingensböck A, Kuster N 2022 IT'IS Database for thermal and electromagnetic parameters of biological tissues. <https://itis.swiss/virtual-population/tissue-properties/overview/>
- [27] NadhPrudhvi B, Madhav B T P, Kumar Siva M, Rao Venkateswara M and Anilkumar T 2019 Circular ring structured ultra-wideband antenna for wearable applications. *Int. J. RF Microw. Comput. Aided Eng.* 29: e21580
- [28] Bhattacharya A, Dasgupta B and Jyoti R 2021 A simple frequency selective surface structure for performance improvement of ultra-wideband antenna in frequency and time domains. *Int. J. RF Microw. Comput. Aided Eng.* 31: e22857
- [29] Pandhare R A, Abegaonkar M P and Dhote C 2022 High gain wideband and multi-band on-demand reconfigurable antenna for modern wireless application. *Int. J. Microw. Wirel. Technol.* 15: 649–664
- [30] Blattenberger K 2019 Dielectric Constant, Strength, & Loss Tangent, *RF cafe.[online] Rfcafe. Com*
- [31] Pandhare R A, Abegaonkar M P and Dhote C 2022 UWB antenna with novel FSS reflector for the enhancement of the gain and bandwidth. *Int. J. Microw. Wirel. Technol.* 14: 1353–1368
- [32] Sugumaran B, Balasubramanian R and Palaniswamy S K 2021 Reduced specific absorption rate compact flexible monopole antenna system for smart wearable wireless communications. *Eng. Sci. Technol. Int. J.* 24: 682–693
- [33] Pandhare R A, Abegaonkar M P and Dhote C 2022 High gain frequency reconfigurable multifunctional antenna for modern wireless and mobile communication systems. *Int. J. RF Microw. Comput. Aided Eng.* 32: e23385
- [34] Kumkhet B, Raklua P, Wongsin N, Sangmahamad P, Thaiwiro W, Mahatthanajatuphat C, Chudpooti N. 2023 SAR reduction using dual band EBG method based on MIMO wearable antenna for WBAN applications. *AEU Int. J. Electron. Commun.* 160: 154525
- [35] Wang M, Yang Z, Wu J, Bao J, Liu J, Cai L, Dang T, Zheng H, Li E. 2018 Investigation of SAR reduction using flexible antenna with metamaterial structure in wireless body area network. *IEEE Trans. Antennas Propag.* 66: 3076–3086
- [36] Ahmad A, Faisal F, Ullah S and Choi D Y 2022 Design and SAR analysis of a dual band wearable antenna for WLAN applications. *Appl. Sci.* 12: 9218

- [37] Zhang HH, Gong LF, Liu XZ, Xu YX, Cheng GS, Liu Y, Shi GM, Zheng C, Han YJ 2023 Design of low-SAR and high on-body efficiency tri-band smartwatch antenna utilizing the theory of characteristic modes of composite PEC-lossy dielectric structures. *IEEE Trans. Antennas Propag.* 71: 1913–1918
- [38] Kissi C, Särestöniemi M, Kumpuniemi T, Myllymäki S, Sonkki M, Srfi MN, Jantunen H, Pomalaza-Raez C 2019 Reflector-backed antenna for UWB medical applications with on-body investigations. *Int. J. Antennas Propag.* 1–17
- [39] Standard, A R I B 1998 Standard Specific Absorption Rate (SAR) Estimation for Cellular Phone, *ARIB STDT56*, Version 1.0, pp. 1–73

Springer Nature or its licensor (e.g. a society or other partner) holds exclusive rights to this article under a publishing agreement with the author(s) or other rightsholder(s); author self-archiving of the accepted manuscript version of this article is solely governed by the terms of such publishing agreement and applicable law.